

Application of Artificial Intelligence to Real-Time Fault Detection in Permanent-Magnet Synchronous Machines

Yaw Nyanteh, *Graduate Student Member, IEEE*, Chris Edrington, *Senior Member, IEEE*, Sanjeev Srivastava, *Senior Member, IEEE*, and David Cartes, *Senior Member, IEEE*

Abstract—This paper discusses faults in rotating electrical machines in general and describes a fault detection technique using artificial neural network (ANN) which is an expert system to detect short-circuit fault currents in the stator windings of a permanent-magnet synchronous machine (PMSM). The experimental setup consists of PMSM coupled mechanically to a dc motor configured to run in torque mode. Particle swarm optimization is used to adjust the weights of the ANN. All simulations are carried out in MATLAB/SIMULINK environment. The technique is shown to be effective and can be applied to real-time fault detection.

Index Terms—Expert system, neural network, particle swarm optimization (PSO), permanent-magnet synchronous machine (PMSM).

I. INTRODUCTION

FAULT detection and diagnosis (FDD) and increasing prognosis are important tools for the reliability, availability, and survivability of marine vessels. Extending the FDD into predictive and prognostic automated equipment awareness increases the value of this technology. Nowadays, the real-time data acquisition, classification, assimilation and correlation, and cognitive mapping functions can be almost completely automated at reasonable cost with modern computer technologies. The rapid development of computer, sensor, and signal processing technologies, together with artificial intelligence (AI) techniques, has made it possible to implement fault diagnosis and prognosis effectively at reasonable prices.

Permanent-magnet synchronous machines (PMSMs) are receiving increasing attention for high efficiency and high performance applications due to the advancement of permanent-magnet materials [1], [2]. With the increased use of PMSM in various industrial applications, efficient online condition monitoring and accurate machine fault diagnosis, for these

Manuscript received August 30, 2011; accepted January 11, 2012. Date of publication March 15, 2013; date of current version May 15, 2013. Paper 2011-PCIC-405, presented at the 2011 IEEE Petroleum and Chemical Industry Technical Conference, Toronto, ON, Canada, September 19–21, and approved for publication in the IEEE TRANSACTIONS ON INDUSTRY APPLICATIONS by the Petroleum and Chemical Industry Committee of the IEEE Industry Applications Society. This work was supported by the Office of Naval Research, USA, under Grant N00014-02-1-0623.

The authors are with the Center for Advanced Power Systems, Florida State University, Tallahassee, FL 32310 USA (e-mail: ynyanteh@fsu.edu; cshedrington@caps.fsu.edu; sanjeev@caps.fsu.edu; dave@eng.fsu.edu).

Color versions of one or more of the figures in this paper are available online at <http://ieeexplore.ieee.org>.

Digital Object Identifier 10.1109/TIA.2013.2253081

machines, are very important. In the published literature on fault diagnosis of electric machines, induction motors have been the primary focus until now, e.g., [3]–[5] and the references therein. However, research work on PMSM diagnosis is gathering speed as more and more PMSMs are considered for high performance applications, such as electric vehicles and ship propulsion systems.

Artificial neural network (ANN) has been proposed as an alternative to traditional linear techniques in system identification of complex systems. System identification involves the experimental determination of the dynamics of a system from an examination of the input/output relationships. Typically, a model structure is selected, model parameters are determined, and the model is simulated for verification and validation with the actual system. Since the introduction of the ANN, it has found applications in very diverse fields. One of its very promising application areas is in system identification. Its advantages include its capability for parallel processing, distributed processing, and efficient nonlinear mapping between inputs and outputs [6]. An ANN is a processing system consisting of a large number of simple highly interconnected processing elements in an architecture inspired by the structure of the cerebral cortex of the brain [7].

Particle swarm optimization (PSO) is an optimization technique that uses the behavior of flocking birds or swarming locusts to stochastically approach the local optimum of a function. Proposed in 1995, this technique has found application in several areas due mainly to its ease of implementation and its resistance to local optimal traps. Since its introduction, the original PSO has undergone modifications aimed at obtaining a good balance between exploitation and exploration of the solution space so that the algorithm is able to avoid local optimal locations while approaching the global best location faster [8].

II. WINDING INSULATION SYSTEMS

A. Organization

The windings of rotating machines are made up of conductors, the winding core, and winding insulation. The winding insulation prevents short circuits between conductors, maintains windings together, and prevents vibration. The winding insulation is also a means of conducting heat to the cooling system. The insulation system, however, adds to the cost of

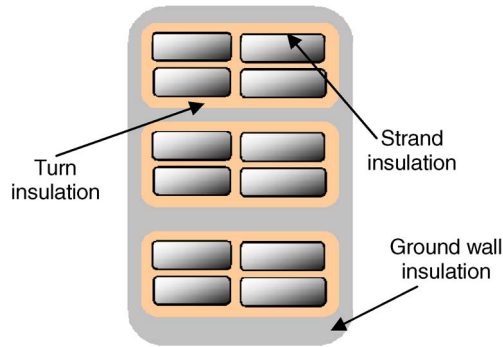


Fig. 1. Winding insulation features.

the machine, increases the weight and size of the machine, and reduces machine efficiency. Fig. 1 shows the main features of winding insulation systems. The types of winding insulation systems are strand insulation, turn insulation, and ground-wall insulation. Strand insulation prevents shorts between different strands of conductors and reduces skin effect on the wire strand. The turn insulation prevents shorts between turns in a winding while the ground-wall insulation separates the grounded machine core from the machine windings. Winding insulation failure is the key electrical failure mechanism [9].

B. Winding Insulation System Testing

Several insulation system designs are tested to determine the best system in terms of cost and performance. Testing determines the expected life of the insulation. An insulation system consists of conductors and insulation materials that provide winding insulation in a machine. The testing methods used in insulation systems are called accelerated aging techniques. These are classified into thermal, electrical, mechanical, and environmental tests based on the type of stress applied on the insulation system. During testing, a candidate system is compared with a reference system whose performance is known [10]. Samples of the candidate system are tested by impressing aging stresses to determine the time to failure. Statistical methods are used to quantify variations between samples of the same insulation system and to also determine an objective basis for comparison of candidate systems to the reference system. The usual definitions of mean and standard deviations apply in these tests. The mean time to failure and standard deviations of the time to failure of a candidate system are given by

$$\tilde{X} = \frac{\sum X_i}{N} \quad (1)$$

$$s = \left[\frac{\sum (X_i - \tilde{X})^2}{N - 1} \right]^{1/2} \quad (2)$$

where

- \tilde{X} mean time to failure;
- X_i sample time to failure;
- s sample standard deviation of time to failure;
- N number of samples of the candidate system.

TABLE I
THERMAL TEST INDUSTRY STANDARDS

Name	Description
ANSI/IEEE Standard No. 1	Recommended Practice for Temperature limits in the rating of electrical equipment and for the evaluation of electrical insulations
IEEE Standard No. 98	Standard for the preparation of test procedures for the thermal evaluation of solid electrical insulation materials
IEEE Standard No. 101	Statistical analysis of thermal life test data
IEC Publication No. 60085	Thermal evaluation and classification of electrical insulation
IEC 60216 Series	Guide for the determination of thermal endurance properties of electrical insulating materials

Statistical distributions are used to model the variations of the data obtained during testing. The lognormal distribution is described by

$$x_i = \log y_i \quad (3)$$

where y_i is the measure value of the stress factor.

The logarithm can be the natural logarithm, or a base ten logarithm can be used. This distribution is used to analyze results in which temperature is a stress factor. Another commonly used statistical distribution is the Weibull distribution given by

$$F(x) = 1 - \exp\left(-\left(t/\alpha\right)^\beta\right) \quad (4)$$

where

- α scale parameter;
- β shape parameter;
- t time.

The distribution determines when a candidate system would fail after time t . Regression analysis is performed to fit curves to determine relationships between stress factors and time to failure and can be used for predictions. Sometimes during testing, candidate systems do not fail, and data censoring techniques are used to account for different samples sizes. Table I lists different types of tests that can be performed on the insulation during design.

C. Types of Tests

Thermal testing establishes the thermal endurance of the insulation system. A so-called thermal endurance plot, which is a graph of the time to failure against the reciprocal of absolute temperature, is determined with this test. The insulation material is then given a temperature index. IEC-accepted temperature indices for different classes of materials are summarized in Table II.

An insulation material breaks down when a high enough voltage is applied across it. This is the short-term breakdown voltage strength. During normal operation of most machines, insulation systems are rarely subjected to short-term breakdown voltages. High frequencies tend to age materials quicker, so voltage endurance tests are carried out at slightly higher than normal voltages and higher frequencies than normal supply

TABLE II
TEMPERATURE CLASSIFICATION FOR INSULATING MATERIALS

Numerical Classification	Letter Classification	Temperature
105	A	105
130	B	130
155	F	155
180	H	180

TABLE III
DISTRIBUTION OF FAILURE PROCESSES FOR ELECTRICAL MACHINES

Component	Percent of motor failures
Bearings	41
Stator	37
Rotor	10
Accessories	12

frequencies. IEEE 1043 gives specific details of voltage endurance testing, but no equivalent IEC standard has been developed.

Thermal cycling, sometimes referred to as load cycling, is caused by frequent load changes which cause current and operating temperatures to cycle abruptly between low and high values. IEEE 1310 and IEC 60034 provide details on the thermal cycling tests. Testing is carried out by applying an ac or dc current through each coil to raise the temperature. The current supply is cut, and the material is allowed to cool. After some time, the current is applied again to raise the temperature. This process is repeated for about 500 times. Two or more stresses can be applied either simultaneously or sequentially at higher levels than that occurring during the normal operation of the machine. These tests that apply to more than one stress are called multifactor tests. Multifactor tests greatly reduce the time to failure. Few standards, IEEE 1064 and IEC 60034, have developed procedures for these tests [11]–[13]. In these tests, the aging stresses are accelerated at a rate so that aging due to all such stresses are the same.

III. FAILURE PROCESSES FOR ELECTRICAL MACHINES

Failure processes can occur as a result of a one-time catastrophic process such as improper electrical winding connections and operating errors. Machine failure can also be gradual due to aging that can be attributed to mechanical and electrical degradation. As aging continues, any or a combination of electrical and mechanical transients can occur to cause the total breakdown of the machine. These include, but not limited to, lightning strikes, operator errors, out-of-phase synchronization, and power supply fault. Table III gives the breakdown of faults in electric machines obtained from EPRI.

The factors which affect particular failure mechanisms are the quality of the winding manufacture, the operating environment of the machine, the past maintenance of the machine, and the quality of the winding. Abrasive particles, oil, moisture, chemicals, ambient temperature, and ambient humidity increase machine degradation. Some mechanisms that gradually lead to stator winding breakdown are thermal deterioration, thermal cycling, loose coils, semiconductive coating failure, inadequate impregnation during insulation manufacturing process, repetitive voltage surges, impurity contamination, chemical attack,

inadequate end-winding spacing, end-winding vibration, and stator coolant water leaks.

A. Thermal Overloading

Overloading a machine can also cause heating through thermal degradation that will slowly eat away at the winding insulation. Other causes of thermal degradation are the design of the stator and rotor, short time between starts and stops, negative sequence currents, dirty windings with abrasive particles, damaged heat exchange tubes, debris or copper oxide, loose coils, underexcited operation of synchronous machines, and rapid cooling and heating of stator coils. Random stator windings that are undergoing breakdown due to thermal deterioration have cracked or peeling magnetic wire films. When insulation resistance test is carried out, the insulation has very little resistance and has a low surge breakdown voltage in the surge voltage test. The dissipation factor increases, and there is a slight increase in capacitance. In form-wound stator windings, there is a decrease in capacitance, increase in power factor, partial discharges, and surface temperature. The stator undergoing thermal breakdown should have its windings and heat exchangers cleaned. Sometimes, depending on the levels of breakdown, a new vacuum pressure impregnation process can be performed. During operation, ensure voltage balance, reduce maximum permissible load, and install protective relays and, in the case of synchronous machines, adjust the power factor. It is also a good idea to upgrade the heat exchanger and install chillers.

B. Thermal Cycling

Thermal cycling occurs when a machine cycles between different load levels at very short intervals. Rapid starts and stops also cause thermal cycling. When the insulation system design is bad, it may not be able to withstand cyclic axial shear stresses. Also, load cycling results in higher temperatures in the stator windings beyond the bonding strength of resins that hold windings together. Some symptoms of thermal cycling are puffy insulation at the core ventilation ducts and outside slots, the insulation feels hollow when tapped, and there are circumferential cracks on the stator windings. Other symptoms can be seen as abrasion in the stator insulation, low insulation resistance, and low polarization index during the polarization test. Once these symptoms start to show, no effective remedial process has been developed. Methods to slow down eventual breakdown include reducing the number of starts and stops, reducing the maximum permissible load, and operation at unity power factor.

C. Repetitive Voltage Surges

Voltage surges are sudden voltage rises beyond the normal voltage rating of the machine. The rise can be about ten times or more than the normal rated voltage. These bursts of voltages are also associated with high frequency in the harmonic contents of the inverter-fed drive (IFD), and this further increases electrical degradation. Some of these transients are lightning, ground faults in the power system, generator breaker operation, IFD,

TABLE IV
OFFLINE STATOR AND ROTOR TESTS

Test	Test
Insulation resistance and polarization index	Stator wedge tap
DC HIPOT	Slot side clearance
AC HIPOT	Stator slot radial clearance
Capacitance test	Stator end-winding resonance
Capacitance tip-up	Rotor voltage drop
Dissipation factor tip-up	Rotor RSO and surge
Power factor tip-up	Rotor growler
Offline partial discharge	Rotor fluorescent dye penetrant
Partial discharge probe	Rotor rated flux
Stator surge comparison	Rotor single-phase rotation
Inductive impedance	Stator blackout test
Semi-conductive coating resistance	Stator pressure and vacuum decay
Conductive coolant tube resistance	

and motor breaker operation. They gradually erode the turn insulation, ground-wall insulation and semiconductive coating, grading coating, and phase insulation. Symptoms of repetitive voltage surges include the presence of ozone and a whitish powder in the magnetic insulation. To correct the degradation due to voltage surges, change the cable length, or replace it with one of higher surge impedance. Install a low-pass filter between the IFD and motor to increase the surge rise time. Install a partial discharge resistant magnetic wire and impregnate stator to reduce voids in insulation and increase the distance between adjacent turns in phase ends.

D. Round and Salient Pole Rotor Failure Processes

Rotor winding degradation is not as prevalent as stator winding degradation. They involve thermal deterioration, thermal cycling, abrasion (due to imbalance), pollution (leading to electrical tracking), repetitive voltage surges, and centrifugal forces. Remedial processes involve replacing the damaged sections or full length of damaged turn insulation, repairing the slot liner, reducing the loading on the machine, cleaning the machine rotor windings, and reducing negative sequence currents. The rate of load changes should be reduced, and copper can be reused or replaced.

E. Wound and Squirrel Cage Induction Machine Rotor Winding Failure Processes

These types of machines can undergo transient overvoltages, unbalanced stator voltages, high resistance connections in bar lap, and wave winding systems. The bandings in the end windings of the wound rotor inductor machines can also give up, and there can be shorting and possible grounding of the slip-ring insulation. With squirrel cage induction machines, the main processes are thermal degradation, thermal cycling, abrasion and pollution, and centrifugal forces. Table IV gives a number of tests that determine the condition of stator and rotor windings together with related IEEE and IEC standards. These tests produce useful information as long as the data are interpreted by a human expert or software system.

TABLE V
ONLINE TEST FOR STATOR AND ROTOR WINDINGS

Test
Thermal monitoring
Condition monitors and tagging compounds
Ozone monitoring
Online partial discharge monitors
End-winding vibration monitors
Synchronous rotor flux monitor
Current signature analysis
Air gap monitoring
Voltage surge monitor
Bearing vibration monitor

IV. CONDITION TESTING AND MONITORING

Machine condition testing is an important aspect of the operation of motor and generators, and over 30 different condition tests have been developed. The time of testing is a downtime, so such tests should be carefully planned. Testing can provide information about faults that have occurred but are not very useful for predicting the time of an impending fault. Testing also looks at the symptoms of a fault and so do not provide information about the root causes of a fault. Another reason for carrying out testing is to determine which machines need maintenance. Commissioning and warranty issues require that a machine meets certain tests to ensure the safety of users. Determining the remaining life of insulation is also difficult with testing since most tests look at the symptoms of a failure process.

Testing can be online and offline. Online testing is sometimes preferred to offline tests since no outage is required. The cost of acquiring diagnostic data is also cheaper than that for offline testing. Online testing can also facilitate predictive maintenance. More importantly, these tests are carried out when voltage, current, and other measured indicators are at their service values. Online testing can also be more expensive since it requires sensors to obtain data. It may also be more complex and may not be applicable to all failure processes. Visual inspections can also be used to assess the condition of a machine. This, however, requires the presence of an expert, the outage of the machine, and the disassembly of the machine in some cases.

A. Online Monitoring for Stator and Rotor Windings

As explained, online testing has more advantages than offline testing. Some of these tests are listed in Table V. For more information on these tests, the references in [14] and [15] can be consulted.

V. FAULT DETECTION IN PMSM

Stator winding faults constitute the bulk of electrical faults in PMSM. Stator winding faults start as incipient turn-to-turn faults, which, if undetected, can cause the total burnout of the entire phase winding. The spreading of turn-to-turn faults takes place in a very short time period. PMSM has gained acceptance in applications where energy density is the major consideration. In such applications, a drive system is designed to control the

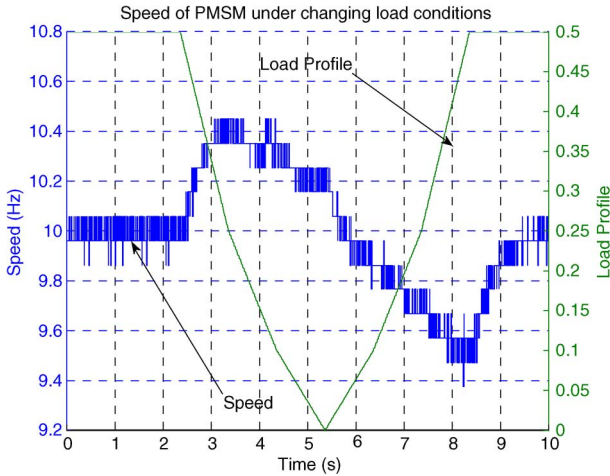


Fig. 2. Speed of PMSM during different loading conditions.

speed of the PMSM. The graph in Fig. 2 shows the variation of speed of a PMSM when supplied from the drive that uses current control to maintain a constant speed. When the loading on the machine increases, the PMSM momentarily loses speed but picks up again when the drive increases current supply. When the loading of the PMSM loading drive decreases, the speed increases until the drive system restores commanded speed again.

This paper provides a detection technique using ANN that can be implemented easily in a real-time digital simulator for the identification of faults in the stator windings of a PMSM. The ANN is trained using PSO to optimize the ANN parameters. The ANN is trained to detect rapid changes in the current supply to the PMSM which, in the experimental setup, is due to short-circuiting of the machine windings. The ANN distinguishes current fluctuations due to load changes because the current rises faster in the case of the short-circuit fault than when it is driving a changing load. A threshold current level is determined based on the frequency of operation of the drive under normal conditions. The ANN is trained for a particular set of machine operating conditions, including drive operating frequency, preset speed command, and a load torque profile. When conditions are changed, the ANN is retrained to enable accurate and optimized performance based on the new operating conditions. PSO is simple to implement and does not require too much computational effort as the genetic algorithm and other stochastic methods. This enables real-time online ANN reconfiguration when operating conditions change as demonstrated in [16]. PSO, however, enables the fast convergence of the ANN parameters for greater accuracy in fault detection.

A. Neural Network Model Development

A neural network with global feedback is shown in Fig. 3. The figure also shows time-tapped delays at each input. The general feedback network with input delays is represented by (5). In the equation, \hat{y} is the output from the representative neural network at different times up to the q th time before

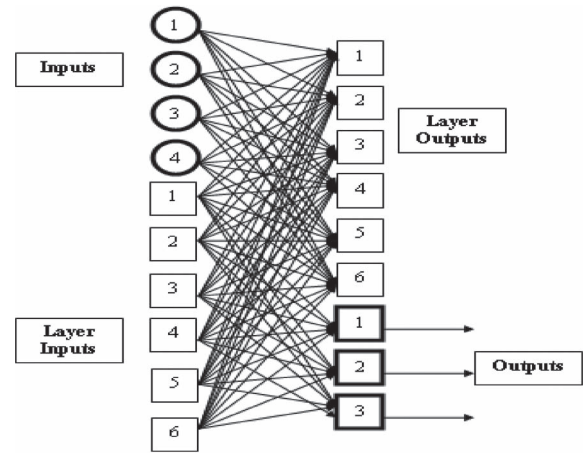


Fig. 3. Structure of a recurrent multilayer ANN.

the current output value, Ω represents the nonlinear functional notation between neural network and output, u is the input at different times up to the p th time before the current time, W is a matrix of the weights of the neural network and other parameters associated with the neural network.

$$\hat{y}(t) = \Omega [\hat{y}(t - 1), \dots, \hat{y}(t - q), (t), u(t - 1), \dots, u(t - p), W] \quad (5)$$

where

- y output of the ANN;
- q time delays of the output;
- Ω nonlinear mapping of output and ANN;
- u input to the ANN;
- p time delays of the input;
- W matrix of ANN weights.

The parameters of the neural network include the weights and biases corresponding to each neuron layer. Time delays give the neural network predictive capabilities, and this can be utilized for fault prognosis. Each neuron layer can be described mathematically by

$$x(k) = \sigma(u, v, b) = \sigma \left(\sum_{r=1}^P \sum_{i=1}^R w_{r,i} \times u_r(k - i + 1) + \sum_{r=1}^G \sum_{j=1}^Q w_{r,j} \times v_j(k - j + 1) + b \right) \quad (6)$$

where

- x time delays of the output;
- u layer input;
- v layer output;
- b layer bias;
- w ANN weights;
- P number of inputs;
- R number of input delays;
- G number of layer outputs;
- Q number of layer output delays.

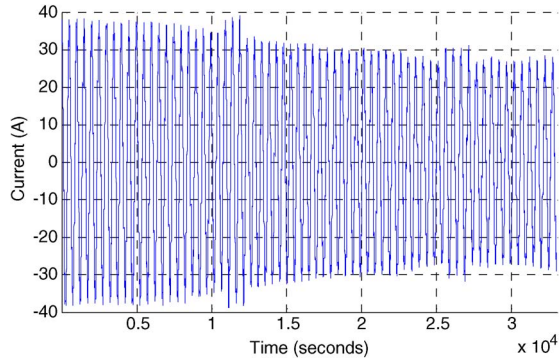


Fig. 4. Phase current for changing load and stator winding fault.

The number of layer delays can be different for each layer, and it is assumed in (6) to be the same for all layers. The choice of activation function is chosen to enable the ANN to quickly learn the patterns in the training data. The options among a host of activation functions include hyperbolic tangent, sinusoidal, and linear functions.

B. ANN Model Training

The detection approach enables the ANN to observe the current wave shape and decide the condition of the PMSM motor. The idea is that a mechanical load change is more gradual than a stator winding defect. Fig. 4 shows this for current in the stator phase A of the PMSM. The current increases for both load increases, but it is very abrupt for the case of a stator winding fault as shown with the rectangles on the graph of Fig. 4. The detection technique should be able to tell when the change in the current level is too abrupt to be a mechanical load change.

Since the current waveform is approximately sinusoidal, running at the frequency of operation of the drive system, the ANN has to compare the peak current value in each period with the maximum value in the subsequent period. If the data points are not approximately sinusoidal, the technique compares a selected current value at an arbitrary point in time to the current value at another point in time separated by a single period of operation of the drive. The ANN is exposed to the current output from the PMSM under changing load conditions from which an envelope is produced around the current output waveform. The envelope function has information about the rise and drop in the current wave shape. Fig. 5 shows an envelope function around the current output. During each period of the current output waveform, the ANN produces an output for each current value. Next, it chooses the maximum output and assigns this value as the ANN perception of the current during that period. The ANN forms an output based on these perceived current values, none of which should be less than the maximum corresponding current value in a given time period based on the frequency of operation of the drive. The weight structure that produces the envelope with the best fit around the current output is chosen for the fault detection.

A variation of PSO is used to systematically update the ANN weight values. PSO does not proceed by the calculation of the gradient of the error function since that may be expensive or,

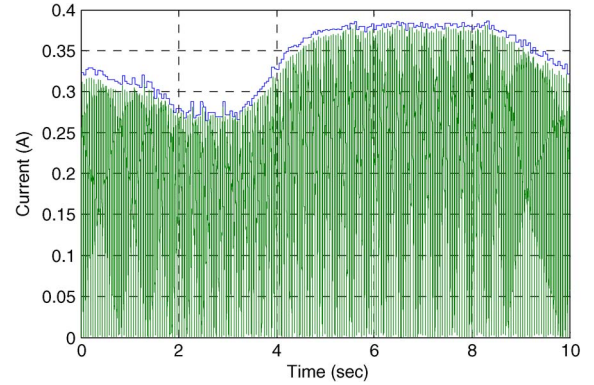


Fig. 5. Plot of current and current envelope.

as discussed, in this case, the cost function is not differentiable. The cost function is given by

$$y_{t=j}^{t=j+T} = \max \left(F_{t=j}^{t=j+T} \right) \quad (7)$$

$$\min \left(\frac{1}{N} \sum_{j=1}^{j=N} y_i \right) \quad (8)$$

where

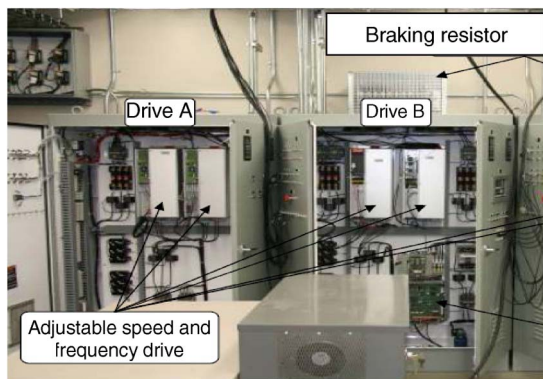
- y ANN output;
- F input during each period;
- \max maximum of ANN output;
- N number of data points.

The cost function forms an envelope around the current output of the PMSM by selecting the maximum output of the ANN during each time period of the input to the ANN. A period starts from time j to $j + T$, where T is the period of operation of the drive. To produce a close fitting envelope around the input to the ANN, the minimum value of the average of y , comprising all N data points, is obtained using PSO as shown in (8). The input to the ANN is the square root of the square of the current value, normalized to fit between 0 and 1, at each time, so only positive values are input to the ANN. The ANN produces a value based on the input at each time that represents its perception of the PMSM current. The y function from these values, however, should be greater than the maximum value of the input at each period. If it is less, PSO applies a penalty to avoid using that weight set. PSO starts by randomly selecting feasible solutions in the solution space called particles. Each particle is then adjusted by

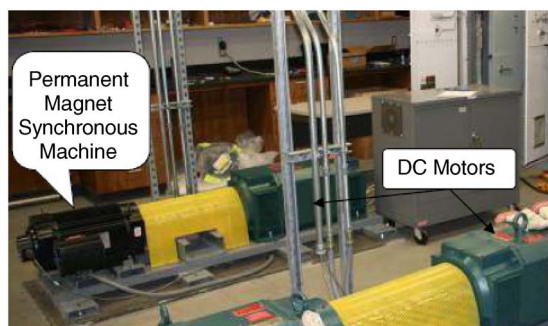
$$\begin{aligned} V_i(k+1) &= W(k)V_i(k) + \text{rand}(0,1)(g\text{best}(k)) \\ &\quad + \text{rand}(0,1)(p\text{best}_i(k)) \\ X_i(k+1) &= X_i(k) + V_i(k+1) \end{aligned} \quad (9)$$

where

- V_i velocity of particle i at time k ;
- W_i inertia weight;
- rand random number between 0 and 1;
- X_i particle i location;
- $g\text{best}$ global best location;
- $p\text{best}_i$ particle i personal best location.



(a)



(b)

Fig. 6. Experimental setup. (a) PMSM drive system. (b) PMSM and dc machine mechanically coupled as load.

The random numbers can be generated from the normal or uniform distribution.

VI. DESCRIPTION OF EXPERIMENTAL SETUP

The experimental setup to obtain data to validate and train the ANN consists of a 28.8-kVA variable frequency drive connected to an 11.25-kW 640-V 60-Hz Y-connected eight-pole PMSM. A dc motor is mechanically coupled to the PMSM to serve as a load. The data acquisition system is developed using a control system interface between the drive system and SIMULINK. This allows the sampling of three phase currents, three phase voltages, fault loop currents, and motor torque data. A speed encoder that provides 60 signals per rotation of the rotor enables the extraction of motor speed values. Fig. 6(a) and (b) shows the experimental setup to simulate fault conditions in the PMSM. The drive system has two drives that supply power and provide speed control of the PMSM. Faults can be simulated in the PMSM by short-circuiting the stator windings in two different locations as shown in Fig. 7. The first location labeled A6-7 to A7-8 applies a short circuit across a full pitch winding while the second location applies a short circuit across half of the windings. These special connections have been made across the A phase of the stator windings.

A. Training Results

The training data comprising the torque loading and the current supply to the PMSM drive are shown in Fig. 8(a).

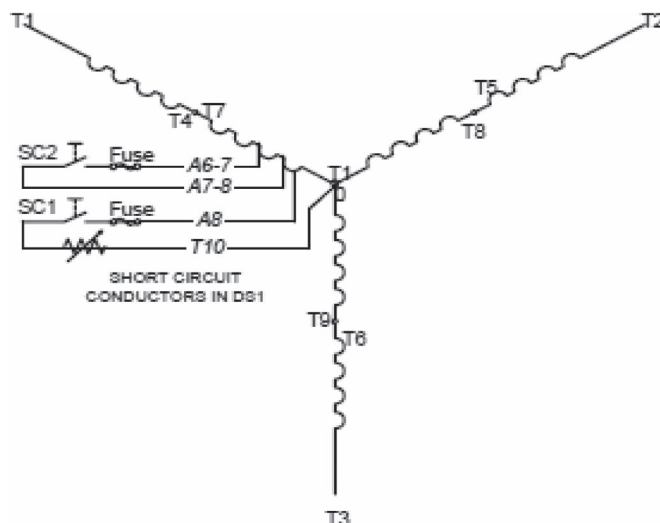


Fig. 7. Circuit diagram for stator short-circuit winding.

The current data, shown in Fig. 8(b), are first processed to ensure that all the data points are positive and between 0 and 1 as shown in Fig. 8(c). In total, the training data consisted of 50 001 input–output data pairs. The training evolution for the ANN based on the PSO method is shown in Fig. 9(a). The evolution shows an average sum of ANN output of 0.3455 after 100 epochs. These results are for the stator phase-A currents. From the second plot of Fig. 9(b), the weight structure stays the same from iteration number 80 to 100. The performance criterion used prevented the use of other methods based on gradient descent. This illustrates the generalizing property of PSO to find optimal solution to nonsmooth objective functions. Other stochastic methods that could have been used are genetic algorithms, simulated annealing, and ant colony. These other optimization methods show comparable performance compared to PSO. PSO was chosen for its simplicity and computational speed when there are too many decision variables; in this case, there were 51 weight parameters.

The actual detection is carried out by finding the changes in the level of the envelope function from one complete cycle to another. This difference in output from one cycle to the next is called a current differential and is expected to be much higher when it is due to short-circuit currents than when it is due to load changes. From results from several training cases, a threshold can be set so that any differential current value above the threshold is considered due to short circuits and any level greater is considered due to noise and load changes.

Fig. 10 shows the performance of the ANN on the training data with and without fault data. It is seen that, for the case of the nonfaulted PMSM [see Fig. 10(a)], there is a slight rise in current as the load starts to increase from 2.5 s. The differential current, however, never rises beyond 0.025. In the faulted case [see Fig. 10(b)], there are distinct peaks at 3.3, 2.85, and 8.85 s well above 0.025. Using the output from the ANN, the time of occurrence of the fault can be detected. Also, the method is able to accurately distinguish between the cases of increasing mechanical load and the case of short-circuited windings. A simple statistical data analysis from a number of fault simulations with PMSM showed that a threshold value of

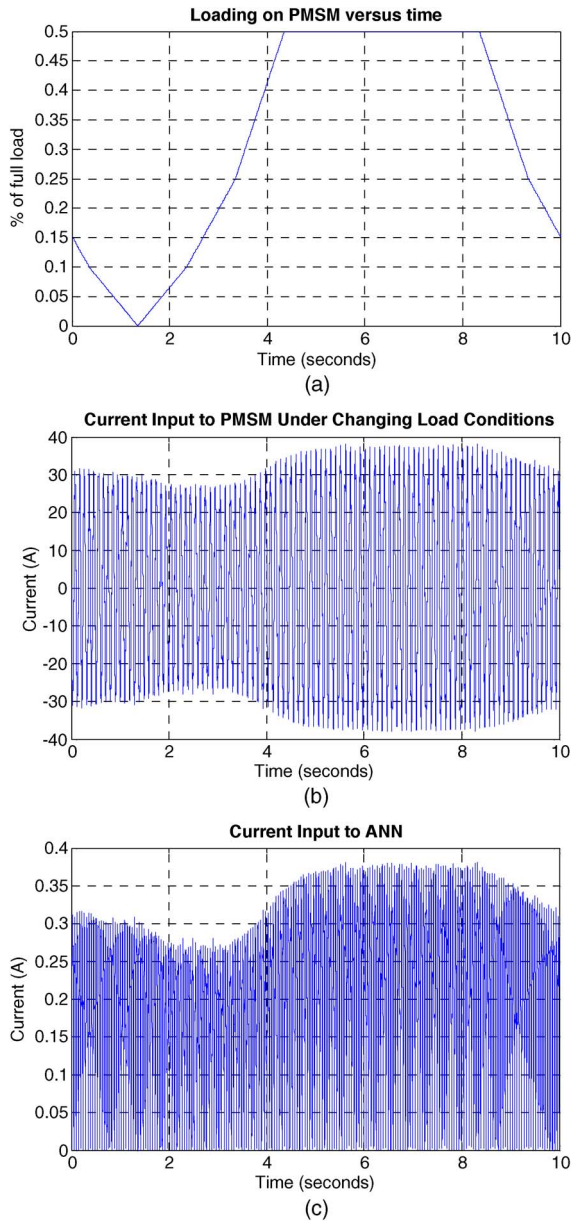


Fig. 8. Training data. (a) Loading on PMSM mechanically connected to dc motor. (b) Current input to PMSM under changing load conditions. (c) Current output after processing.

0.025 represents about 3 standard deviations from the mean ANN for the nonfaulted case. Thus, all values within this threshold are nonfaulted values, and values well above this threshold are fault data. Fig. 10(c) and (d) shows the current at 50% loading for no-fault and fault cases, respectively.

B. Fault Simulation Results

The generalizing ability of the ANN was tested by applying different loadings on the PMSM and is shown in Fig. 11. The result for the 30% full loading condition is shown in Fig. 11. The figure shows how the ANN distinguishes between the PMSM under loading and fault conditions. It is seen that, for the nonfaulted case [see Fig. 11(a)], the current differential is within 0.02 while the faulted case [see Fig. 11(b)] has current

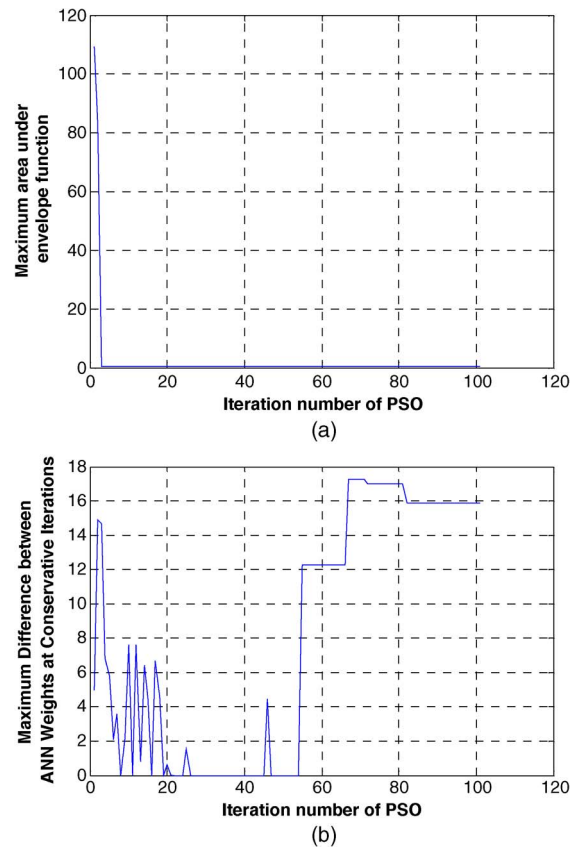


Fig. 9. Training for ANN based on PSO. (a) Training evolution showing the smallest area of envelope function at each iteration of the PSO algorithm. (b) Training evolution showing maximum weight difference.

differentials well above 0.025. This procedure can be used to discriminate between the PMSM under different conditions other than stator fault currents by setting a threshold differential current value. Fig. 10(c) and (d) shows the current at 30% loading for no-fault and fault cases, respectively.

VII. CONCLUSION

The results shown in this paper show a promising technique applicable to real-time FDD. The frequency of operation of the drive can be adjusted to other frequencies other than 10 Hz which was the frequency of operation of the drive in this paper. By the data manipulations discussed, the ANN requires about 0.05 s, in the case of operation at 10 Hz, to make a decision. If the frequency is increased to 60 Hz, the ANN requires 0.00833 s to make decisions. These short time intervals would prevent further damage to the winding of the machine. The simulations have been carried out for values of the ANN output within a threshold range of 3 standard deviations about the sample mean. The threshold can be increased to prevent false alarms. The technique also accurately distinguishes short-circuit faults from loading transients.

PMSM has a number of advantages over induction machines, the most important of which are its high power density and efficiency. PMSMs have been proposed as the propellers of choice in the notional all-electric ship which is still under development under the Electric Ship Research Development

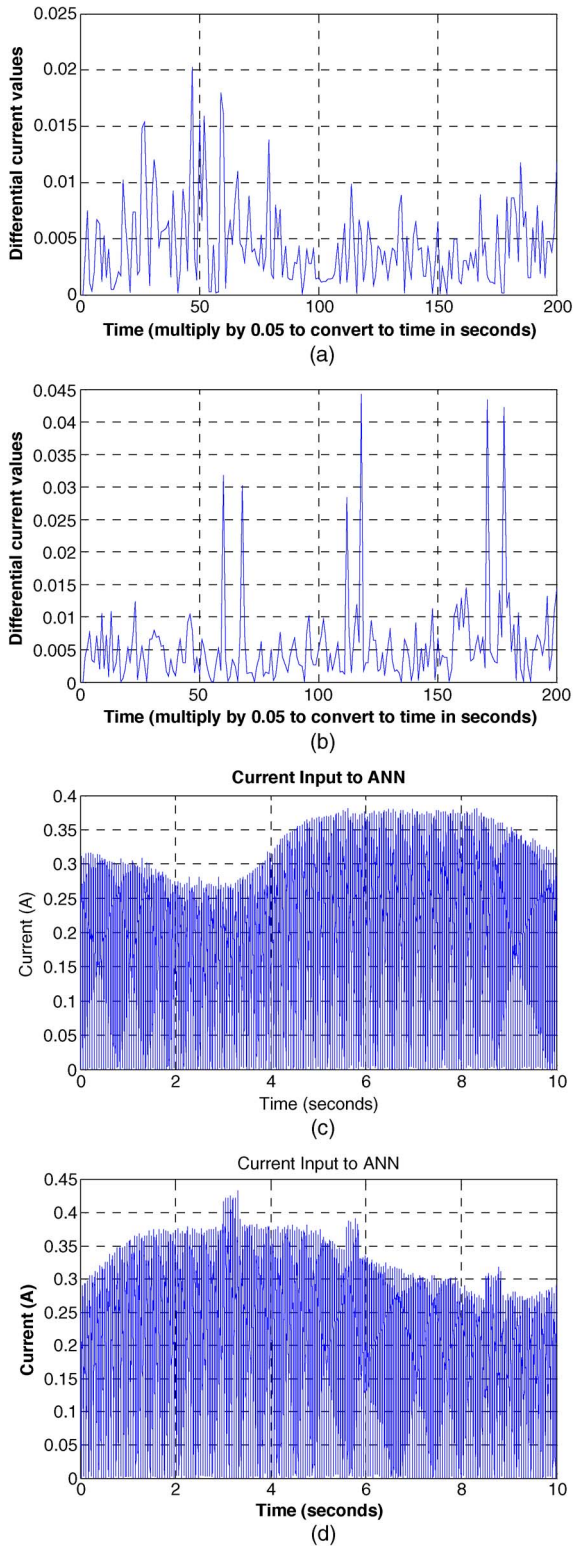


Fig. 10. Comparing the ANN for faulty and nonfaulted PMSMs running at 50% full loading. (a) Output for nonfaulted case. (b) Output for faulted case. (c) Current at 50% loading with no fault. (d) Current at 50% loading with fault.

Consortium. Since the early 1990s, when ANN was introduced as the main AI technique to revolutionize the monitoring and pattern detection techniques in electric machines and power industry, there have been many effort to introduce more AI techniques.

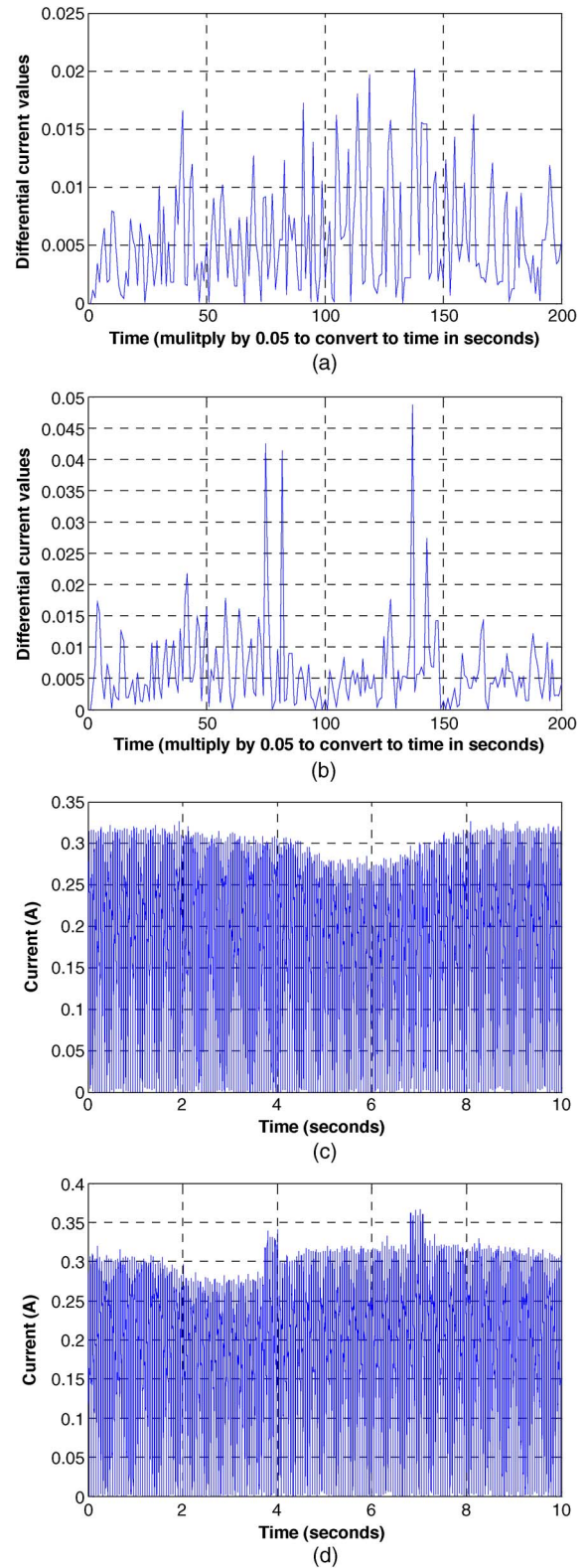


Fig. 11. Conditions at 30% full loading. (a) Output for nonfaulted case. (b) Output for faulted case. (c) Current at 30% loading with no fault. (d) Current at 30% loading with fault.

This paper proposes the use of PSO to enhance the convergence of ANN weight. This technique has been developed into an online monitoring tool developed in hardware for the real-time reconfiguration of ANN parameters due to changes in system configuration of the drive system.

REFERENCES

- [1] M. A. Rahman and P. Zhou, "Analysis of brushless permanent magnet synchronous motors," *IEEE Trans. Ind. Electron.*, vol. 43, no. 2, pp. 256–267, Apr. 1996.
- [2] Y. Kano, K. Tonogi, T. Kosaka, and N. Matsui, "Torque-maximizing design of double-stator, axial-flux, PM machines using simple nonlinear magnetic analysis," in *Conf. Rec. 42nd IEEE IAS Annu. Meeting*, Sep. 2007, pp. 875–881.
- [3] F. Filippetti, G. Franceschini, C. Tassoni, and P. Vas, "Recent developments of induction motor drives fault diagnosis using AI techniques," *IEEE Trans. Ind. Electron.*, vol. 47, no. 5, pp. 994–1004, Oct. 2000.
- [4] S. M. A. Cruz and A. J. M. Cardoso, "Multiple reference frames theory: A new method for the diagnosis of stator faults in three-phase induction motors," *IEEE Trans. Energy Convers.*, vol. 20, no. 3, pp. 611–619, Sep. 2005.
- [5] S. M. A. Cruz and A. J. M. Cardoso, "Diagnosis of stator inter-turn short circuits in DTC induction motor drives," *IEEE Trans. Ind. Appl.*, vol. 40, no. 5, pp. 1349–1360, Sep./Oct. 2004.
- [6] M. A. Rahman and M. A. Hoque, "On-line adaptive artificial neural network based vector control of permanent magnet synchronous motors," *IEEE Trans. Energy Convers.*, vol. 13, no. 4, pp. 311–318, Dec. 1998.
- [7] L. H. Tsoukalas and R. E. Uhrig, *Fuzzy and Neural Approaches in Engineering*. Hoboken, NJ, USA: Wiley, 1997, ser. Wiley Series on Adaptive and Learning Systems for Signal Processing, Communications and Control.
- [8] L. Su-Hua, W. Yao-Wu, X. Xin-Yin, and T. Guang-Yu, "A parallel PSO approach to multi-objective reactive power optimization with static voltage stability consideration," in *Proc. IEEE/PES Transm. Distrib. Conf.*, 2006, pp. 172–176.
- [9] R. Brutsch and M. Chapman, "Insulating systems for high voltage rotating machines and reliability considerations," in *Proc. IEEE Int. Symp. Elect. Insul.*, 2010, pp. 1–5.
- [10] G. C. Stone, E. A. Boutler, I. Culbert, and H. Dhirani, *Electrical Insulation for Rotating Machines*. Hoboken, NJ, USA: Wiley-IEEE Press, 2004, ser. IEEE Series on Power Engineering.
- [11] P. Paloniemi, "Theory of equalizing of thermal aging processes of electrical insulating materials in thermal endurance tests," *IEEE Trans. Electr. Insul.*, vol. EI-16, no. 1, pp. 1–6, Feb. 1981.
- [12] P. Paloniemi, "Theory of equalizing of thermal aging processes of electrical insulating materials in thermal endurance tests," *IEEE Trans. Electr. Insul.*, vol. EI-16, no. 1, pp. 7–17, Feb. 1981.
- [13] P. Paloniemi, "Theory of equalizing of thermal aging processes of electrical insulating materials in thermal endurance tests," *IEEE Trans. Electr. Insul.*, vol. EI-16, no. 1, pp. 18–30, Feb. 1981.
- [14] B. A. Lloyd, G. C. Stone, and J. Stein, "Motor insulation condition assessment using expert systems software," in *Proc. Pulp Paper Ind. Tech. Conf.*, 1994, pp. 60–67.
- [15] A. J. Gonzalez, R. L. Osborne, C. T. Kemper, and S. Lowenfeld, "On-line diagnosis of turbine-generators using artificial intelligence," *IEEE Power Eng. Rev.*, vol. PER-6, no. 6, p. 42, Jun. 1986.
- [16] W. Lui, L. Liu, and D. A. Cartes, "Efforts on real-time implementation of PSO based PMSM parameter identification," in *Proc. IEEE Power Energy Soc. Gen. Meet.*, 2008, pp. 1–7.



Yaw Nyanteh (S'10) received the B.S. degree in electrical and electronics engineering from the University of Science and Technology, PMB Kumasi, Ghana, in 2005 and the M.Sc. degree from the Industrial Engineering Department, Florida State University, Tallahassee, FL, USA, in 2009, where he is currently working toward the Ph.D. degree.

He is a Research Assistant in the Center for Advanced Power Systems at Florida State University.



Chris Edrington (S'94–M'04–SM'09) received the Ph.D. degree in electrical engineering from the University of Missouri-Rolla, Rolla, MO, USA, in 2004.

From 2004 to 2007, he was an Assistant Professor of Electrical Engineering in the College of Engineering at Arkansas State University, Jonesboro, AR, USA. He is currently an Assistant Professor of Electrical and Computer Engineering with the Florida Agricultural and Mechanical University-Florida State University College of Engineering, Tallahassee, FL, USA, and is a Research

Associate for the Florida State University Center for Advanced Power Systems.



Sanjeev Srivastava (S'01–M'04–SM'10) received the Ph.D. degree in electrical engineering from Texas A&M University, College Station, TX, USA, in 2003.

He is an Assistant Scholar Scientist in the Center for Advanced Power Systems at Florida State University, Tallahassee, FL, USA.



David Cartes (S'97–A'99–M'03–SM'07) received the Ph.D. degree in engineering science from Dartmouth College, Hanover, NH, USA.

He has been an Associate Professor with the Department of Mechanical Engineering at Florida State University (FSU), Tallahassee, FL, USA, since January 2001. He is also the Director of the Institute for Energy Systems, Economics and Sustainability at FSU. In 1994, he completed a 20-year U.S. Navy career.